

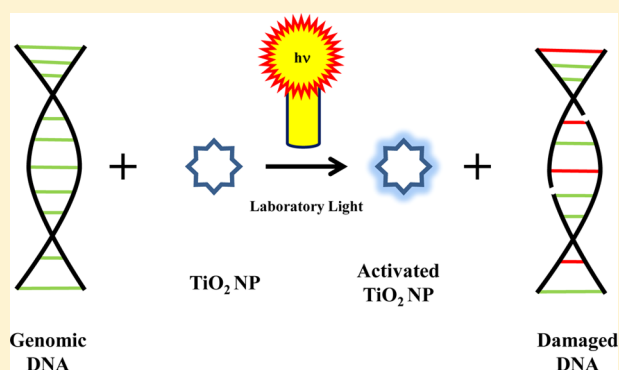
## DNA Damaging Potential of Photoactivated P25 Titanium Dioxide Nanoparticles

Elijah J. Petersen,<sup>†</sup> Vytas Reipa,<sup>†</sup> Stephanie S. Watson,<sup>§</sup> Deborah L. Stanley,<sup>§</sup> Savelas A. Rabb,<sup>‡</sup> and Bryant C. Nelson<sup>\*†</sup>

<sup>†</sup>Material Measurement Laboratory—Biosystems and Biomaterials Division, <sup>‡</sup>Material Measurement Laboratory—Chemical Sciences Division, <sup>§</sup>Engineering Laboratory—Materials and Structural Systems Division, National Institute of Standards and Technology, 100 Bureau Drive, Gaithersburg, Maryland 20899, United States

### Supporting Information

**ABSTRACT:** Titanium dioxide nanoparticles (TiO<sub>2</sub> NPs) are found in numerous commercial and personal care products. Thus, it is necessary to understand and characterize their potential environmental health and safety risks. It is well-known that photoactivated TiO<sub>2</sub> NPs in aerated aqueous solutions can generate highly reactive hydroxyl radicals ( $\bullet$ OH), which can damage DNA. Surprisingly, recent *in vitro* studies utilizing the comet assay have shown that nonphotoactivated TiO<sub>2</sub> NPs kept in the dark can also induce DNA damage. In this work, we utilize stable isotope-dilution gas chromatography/tandem mass spectrometry to quantitatively characterize the levels and types of oxidatively generated base lesions in genomic DNA exposed to NIST Standard Reference Material TiO<sub>2</sub> NPs (Degussa P25) under precisely controlled illumination conditions. We show that DNA samples incubated in the dark for 24 h with TiO<sub>2</sub> NPs (0.5–50  $\mu$ g/mL) do not lead to the formation of base lesions. However, when the same DNA is exposed to either visible light from 400 to 800 nm (energy dose of  $\sim$ 14.5 kJ/m<sup>2</sup>) for 24 h or UVA light at 370 nm for 30 min (energy dose of  $\sim$ 10 kJ/m<sup>2</sup>), there is a significant formation of lesions at the 50  $\mu$ g/mL dose for the visible light exposure and a significant formation of lesions at the 5 and 50  $\mu$ g/mL doses for the UVA light exposure. These findings suggest that commercial P25 TiO<sub>2</sub> NPs do not have an inherent capacity to oxidatively damage DNA bases in the absence of sufficient photoactivation; however, TiO<sub>2</sub> NPs exposed to electromagnetic radiation within the visible portion of the light spectrum can induce the formation of DNA lesions. On the basis of these findings, comet assay processing of cells exposed to TiO<sub>2</sub> should be performed in the dark to minimize potential artifacts from laboratory light.



### INTRODUCTION

Engineered titanium dioxide nanoparticles (TiO<sub>2</sub> NPs) are found in numerous commercial and personal care products.<sup>1</sup> Many of the personal care products, such as over-the-counter sunscreen creams and/or aerosolized sunscreen sprays, are used by large segments of the population (adults and children). Characteristic exposure routes for TiO<sub>2</sub> NP-containing personal care products can include either skin adsorption or lung inhalation, depending on the product formulation. Thus, it is necessary to understand and characterize the potential environmental and biological effects posed by these NPs.

It is well-known that photoactivated TiO<sub>2</sub> NPs can generate highly reactive hydroxyl radicals ( $\bullet$ OH) in aerated aqueous solutions and superoxide radical anions (O<sub>2</sub><sup>•-</sup>) in non-aqueous media.<sup>2</sup> The mechanisms for the formation of  $\bullet$ OH from photoactivated TiO<sub>2</sub> NPs in solution have been investigated and documented extensively<sup>2–5</sup> and will not be reiterated here. However, once formed,  $\bullet$ OH can interact with and damage various biological molecules, such as DNA, at diffusion-limited rates, resulting in the formation of oxidatively induced DNA

damage (e.g., strand breaks, DNA base and sugar lesions, and abasic sites).<sup>6</sup> The single cell gel electrophoresis assay (alkaline comet assay) is commonly used to measure and characterize NP-induced DNA damage (single-strand breaks, SSBs).<sup>4</sup> When the comet assay specifically incorporates the use of DNA glycosylases or DNA endonucleases such as *Escherichia coli* formamidopyrimidine DNA glycosylase (Fpg) or *E. coli* endonuclease (III) (EndoIII) into the assay procedure, the observed SSBs predominantly correspond to the presence of oxidatively modified purine or pyrimidine DNA base lesions, respectively.

Many *in vitro* studies have shown, using the comet assay, that photoactivated TiO<sub>2</sub> NPs can indeed induce oxidative damage to DNA in the form of SSBs.<sup>7–9</sup> Surprisingly, numerous recent *in vitro* studies, using the comet assay, have shown that purportedly nonphotoactivated TiO<sub>2</sub> NPs (NPs exposed to cells in the dark or to cells under ambient (visible) laboratory

Received: August 20, 2014

light) can also induce significant levels of SSBs.<sup>10–15</sup> Other recent *in vitro* studies report no statistically significant formation or accumulation of SSBs when exposures occur in the dark or under normal ambient laboratory lighting conditions.<sup>16,17</sup> Thus, the inherent capacity of TiO<sub>2</sub> NPs to induce oxidative damage to DNA without photoactivation is unclear. Importantly, the capacity of using the comet assay to characterize and accurately measure the purported DNA damage from TiO<sub>2</sub> NPs has also been seriously questioned as a result of false-positive results,<sup>18</sup> a finding similar to an earlier study suggesting an artifact in the comet assay with germanium nanoparticles.<sup>19</sup> In the Rajapakse et al. study,<sup>18</sup> the authors concluded that many of the false-positive comet assay results were due to the TiO<sub>2</sub> NPs directly interacting *post festum* with the DNA to produce exaggerated comet tails. Overall, determining the DNA damaging potential of photoactivated TiO<sub>2</sub> NPs has been complicated by the large variety of cellular exposure models utilized in previous studies, insufficient physicochemical characterization of the tested NPs, discrepancies in NP dispersion procedures, and uncontrolled or unreported lighting conditions utilized during the testing procedures.

In this fundamental, molecular level investigation, we utilize high-resolution, stable isotope-dilution gas chromatography/tandem mass spectrometry (GC/MS/MS) to quantitatively characterize the levels and discriminate among the types of oxidatively generated DNA base lesions. Advantages of the isotope-dilution mass spectrometry approaches have been recently described at length<sup>4</sup> and have been successfully used in several recent nanogenotoxicity studies by our group.<sup>20–24</sup> Genomic DNA samples were analyzed using GC/MS/MS after direct exposure to well-characterized National Institute of Standards and Technology (NIST) Standard Reference Material (SRM) TiO<sub>2</sub> NPs (SRM 1898, which was made using Degussa P25) under three controlled illumination conditions: darkness, visible light, and ultraviolet A (UVA) radiation. While other studies have been performed using plasmid DNA and/or calf thymus DNA (ct-DNA) exposed to illuminated TiO<sub>2</sub> NPs,<sup>8,9,25–28</sup> this is the only study, to our knowledge, that clearly identifies and quantifies specific mutagenic and cytotoxic DNA base lesions resulting from exposure to varying TiO<sub>2</sub> NP concentrations and precisely controlled light irradiation.

## MATERIALS AND METHODS

**Reagents and Consumables.** Nitrilotriacetic acid disodium salt (NTA), iron chloride (FeCl<sub>3</sub>), 30% (volume fraction) hydrogen peroxide (H<sub>2</sub>O<sub>2</sub>), hydrochloric acid (99.99% purity), ct-DNA (sodium salt), sodium phosphate monobasic, and sodium phosphate dibasic were obtained from Sigma-Aldrich (St. Louis, MO). Internal standards 4,6-diamino-5-formamidopyrimidine-<sup>13</sup>C,<sup>15</sup>N<sub>2</sub> (Fapy adenine-<sup>13</sup>C,<sup>15</sup>N<sub>2</sub>), 2,6-diamino-4-hydroxy-5-formamidopyrimidine-<sup>13</sup>C,<sup>15</sup>N<sub>2</sub> (Fapy guanine-<sup>13</sup>C,<sup>15</sup>N<sub>2</sub>), 8-hydroxyadenine-<sup>15</sup>N<sub>5</sub> (8-OH-adenine-<sup>13</sup>C,<sup>15</sup>N<sub>2</sub>), 5-hydroxy-5-methylhydantoin-<sup>13</sup>C,<sup>15</sup>N<sub>2</sub> (5-OH-5-Me-Hyd-<sup>13</sup>C,<sup>15</sup>N<sub>2</sub>), and 8-hydroxy-2'-deoxyguanosine-<sup>15</sup>N<sub>5</sub> were purchased from Cambridge Isotope Laboratories (Andover, MA). 8-Hydroxyguanine-<sup>15</sup>N<sub>5</sub> (8-OH-guanine-<sup>15</sup>N<sub>5</sub>) was obtained by hydrolysis of 8-hydroxy-2'-deoxyguanosine-<sup>15</sup>N<sub>5</sub> with 60% formic acid at 140 °C for 30 min followed by lyophilization. Subsequently, 8-OH-guanine-<sup>15</sup>N<sub>5</sub> was dissolved in 10 mM NaOH before use. *E. coli* formamidopyrimidine DNA glycosylase (Fpg) and *E. coli* endonuclease (III) (EndoIII) were purchased from Trevigen (Gaithersburg, MD). NIST SRM 1898 (P25 TiO<sub>2</sub> NP) was obtained from the NIST Standard Reference Materials Program. Chelex 100 resin was purchased from BioRad Laboratories (Hercules, CA). Plastic UV-transparent spectrophotometric cuvettes were purchased from Sigma

(St. Louis, MO). Microcon Ultracel YM-30 centrifugal filters (30 kDa molecular weight cutoff) were obtained from Millipore (Billerica, MA). Distilled and deionized water (ddH<sub>2</sub>O), obtained from a Waters Milli-Q system, was used to prepare all aqueous solutions.

**Nanoparticle Characterization.** The TiO<sub>2</sub> NP powder (SRM 1898) used in this study was formed from AEROXIDE TiO<sub>2</sub> P25 powder obtained from Evonik Degussa GmbH, Germany. SRM 1898 has been extensively characterized physically and chemically<sup>29,30</sup> and has been established, for example, to have a specific surface area (multipoint BET) of 55.55 ± 0.70 m<sup>2</sup>/g, a relative phase fraction (X-ray diffraction) of 0.76 ± 0.03 (anatase) and 0.24 ± 0.03 (rutile), and a particle suspension size in PBS (laser diffraction spectroscopy) of 75 ± 4 nm. The errors in the specific surface area and relative phase fraction measurements represent expanded uncertainties about the mean values, and the error in the particle size measurement represents the approximate 95% confidence interval about the mean value.

**Preparation of Nanoparticle Dispersions.** A stock solution (10 mg/mL) of TiO<sub>2</sub> NPs in ddH<sub>2</sub>O was prepared using a standardized sonication method previously described.<sup>30</sup> NP suspensions were prepared by sonication using a Branson 450 analogue sonicator (Branson Ultrasonics Corp., Danbury, CT) for 15 min in 80% pulsation mode and with a sonication power of ≈50 W. This approach follows a standardized dispersion protocol using a calibrated ultrasonicator.<sup>30</sup> The particle size distribution was analyzed initially and every time a DNA damage experiment was initiated using laser diffraction spectrometry (LDS) (Partica LA-950 V2; Horiba Instruments Inc., Irvine, CA).

**Preparation of ct-DNA Stock Solutions and Positive Controls.** Calf thymus DNA stock solutions (500 mg/L) were prepared by dissolving the appropriate amount of ct-DNA in ddH<sub>2</sub>O. Transition metals and other impurities were removed by treating the ct-DNA solutions with Chelex resin combined with extensive dialysis (3500 Da MWCO membranes) against ddH<sub>2</sub>O at 4 °C.<sup>31</sup> Calf thymus DNA stock solutions were stored at 4 °C until needed. Positive control ct-DNA (Fenton chemistry damaged) was prepared using NTA, FeCl<sub>3</sub>, and H<sub>2</sub>O<sub>2</sub> as previously described.<sup>31</sup> The positive control ct-DNA samples were prepared in 100 μg aliquots, dried (SpeedVac), and stored at 4 °C until needed. Positive controls were resolubilized with ddH<sub>2</sub>O (gentle shaking at 4 °C for 24 h) and run with every set of samples to verify sample preparation procedures and instrument performance.

**Protocol for Dark Exposure Studies.** A 250 mg/L TiO<sub>2</sub> NP suspension was prepared by volumetrically diluting the 10 mg/mL TiO<sub>2</sub> NP stock solution with ddH<sub>2</sub>O. A 100 mmol/L phosphate buffer solution (pH 7.4) was prepared by appropriately combining monobasic and dibasic phosphate salts in ddH<sub>2</sub>O. After utilizing Chelex resin to remove transition metal impurities, the pH of the phosphate buffer was adjusted using HCl. The following step was conducted in a darkened laboratory with no exterior sunlight. Appropriate volumes of the 100 mmol/L phosphate buffer solution, the 500 mg/L ct-DNA stock solution, and the 250 mg/L TiO<sub>2</sub> NP solution were added into UV opaque amber 2 mL microfuge vials (Eppendorf) to make 1 mL samples containing 5 mmol/L phosphate buffer, 250 μg ct-DNA, and increasing TiO<sub>2</sub> NP concentrations (0.5, 5, and 50 mg/L). Negative controls without TiO<sub>2</sub> NPs were prepared similarly. Five or six samples were prepared per condition. All of the samples were incubated at 37 °C on a rotating (100 rpm) shaker (C24 Incubator Shaker, New Brunswick Scientific) for 3 or 24 h. After the exposure period, the samples were first centrifuged at 15 700g for 1 h at 4 °C to pellet the TiO<sub>2</sub> NPs. Preliminary experiments based on digestion of test samples with hydrofluoric acid and analysis with inductively coupled plasma–optical emission mass spectrometry (ICP–OES) indicated that 97.8 ± 1.4% of the TiO<sub>2</sub> NPs were removed by centrifugation under these conditions (see Supporting Information for additional details). This high TiO<sub>2</sub> NP removal efficiency indicated that any remaining TiO<sub>2</sub> NPs in the sample were unlikely to cause additional damage to the DNA during subsequent experimental steps. Next, 500 μL of the sample supernatant (containing the ct-DNA) was transferred into a 30 kDa centrifugal filter unit and centrifuged at 15 700g for at least 15 min at 20 °C.

Another 400  $\mu\text{L}$  of ddH<sub>2</sub>O was then added to the top of the filtration membrane and washed through by centrifuging at 15 770g for at least an additional 15 min at 20 °C. To resolubilize the DNA for quantification, another 400  $\mu\text{L}$  of ddH<sub>2</sub>O was added to the top of the filtration membrane, and the filter was capped and stored at 4 °C for  $\geq 24$  h. After this period, the samples were reverse-eluted by centrifugation at 3000g for 5 min at 20 °C into clean 1.5 mL clear Eppendorf tubes and stored at 4 °C for  $\leq 24$  h. The DNA concentration in each sample was determined by spectrophotometric absorbance at 260 nm (absorbance of 1 = 50  $\mu\text{g}$  of double-stranded DNA/mL). Fifty micrograms of DNA was added into clean Eppendorf tubes along with all of the stable isotopically labeled DNA lesion analogues (excluding 8-OH-guanine) and dried under vacuum. All samples were stored with desiccant at 4 °C until enzymatic digestion. Prior to enzymatic digestion and GC/MS/MS analysis (below), isotopically labeled 8-OH-guanine was added to all of the samples. All samples were stored with desiccant at 4 °C until enzymatic digestion. Even though the determination of oxidatively induced DNA damage via GC/MS procedures has been designed and optimized to minimize artifactual formation of 8-OH-guanine,<sup>32</sup> an additional experiment was performed to confirm the lack of artifactual 8-OH-guanine formation. We prepared an additional set of exposure samples incubated for 24 h in the dark with and without TiO<sub>2</sub> NPs and analyzed these samples for 8-OH-deoxyguanosine levels by LC/MS/MS<sup>22</sup> (see Supporting Information for LC/MS/MS method details) and for 8-OH-guanine levels by GC/MS/MS.

**Protocol for Visible Light Exposure Studies.** This study was designed to simulate lighting conditions in a laboratory under normal operating conditions. Illumination experiments were conducted at 37 °C by exposing DNA samples to a table top fluorescent lamp positioned  $\sim 1$  ft. (0.3 m) above the sample holder (a beaker). Exposures were performed using only the visible portion of the electromagnetic radiation spectrum (400–800 nm, Figure 1). Samples

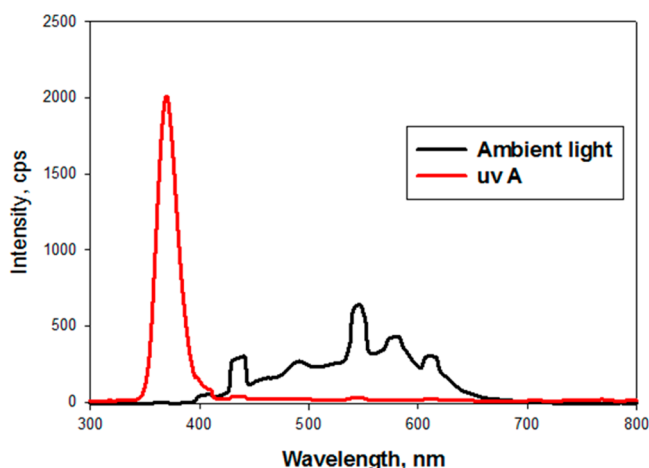


**Figure 1.** Spectral intensities of ambient light and UVA light irradiation utilized in the study.

were contained in plastic UV transparent cuvettes freely floating in a water bath, equilibrated at 37 °C. Light exposure was monitored using an optical fiber inserted into one of the cuvettes and connected to an Ocean Optics Chem2000 fiber optic spectrometer. The spectrometer detector was calibrated for the absolute photon flux by exposing the optical fiber end to the opening in the integrating sphere of the NIST calibrated halogen lamp (Supporting Information, Figure S1). Importantly, light flux was measured continuously during sample exposure, and the total photon flux reaching the samples inside the cuvettes was calculated using a calibration curve. Following setup of the exposure system, a complete set of TiO<sub>2</sub> NP/ct-DNA samples was prepared as described previously for the dark exposure studies except that precautions were not taken to limit laboratory light during sample preparation. Then, the samples were exposed to visible radiation for 24

h to yield a total dose of 14.5 kJ/m<sup>2</sup>. After the exposure period, the samples were centrifuged at 15 700g for 1 h at 4 °C to pellet the TiO<sub>2</sub> NPs and processed as described previously for the dark studies. Each of the 50  $\mu\text{g}$  ct-DNA exposure samples was stored with desiccant at 4 °C until enzymatic digestion.

**Protocol for UVA Light Exposure Studies.** This study was designed to simulate lighting conditions representative of irradiant energy levels in typical sunlight. A UVA wavelength (370 nm, Figure 1) was selected that was less than the band gap ( $\sim 400$  nm) for TiO<sub>2</sub>.<sup>2</sup> Illumination experiments were conducted at 37 °C by exposing DNA samples to black UV lamp light inside a UV reactor (Rayonet, Southern New England Ultraviolet Company). A lamp spectral profile is shown in Figure 1. Samples were contained in plastic disposable UV transparent cuvettes freely floating in water, equilibrated at 37 °C. The light flux (10.0 kJ/m<sup>2</sup>) through the duration of the sample exposures was carefully controlled and quantified as described above. Following setup of the exposure system, a complete set of TiO<sub>2</sub> NP/ct-DNA samples was prepared as described previously for the dark exposure studies. Then, the samples were exposed to UVA radiation for 30 min. After the exposure period, the samples were centrifuged at 15 700g for 1 h at 4 °C to pellet the TiO<sub>2</sub> NPs and processed as described previously for the dark studies. Each of the 50  $\mu\text{g}$  ct-DNA exposure samples was stored with desiccant at 4 °C until enzymatic digestion.

**Enzymatic Digestion and GC/MS/MS Analysis of Exposure Samples.** All samples were enzymatically digested and analyzed via GC/MS/MS methodology based on procedures described in previous studies.<sup>20,21,23</sup> Full details of the methodology are available in the Supporting Information. Briefly, the samples were dissolved in an aqueous buffer and then treated with *E. coli* Fpg and EndoIII DNA deglycosylases. The reaction was stopped by addition of ice-cold ethanol, and the excised DNA lesions (Figure 2) were isolated from undamaged DNA by centrifugation. The samples were trimethylsilylated and analyzed using isotope-dilution GC/MS/MS in the multiple reaction monitoring (MRM) mode.

**Electron Paramagnetic Spectroscopy (EPR) Spin-Trapping Experiments.** TiO<sub>2</sub> NP samples at a concentration of 50 mg/L were prepared in amber microfuge vials with ct-DNA and phosphate buffer identical to the previously described DNA damage experiments, except that 3-amino-2,2,5,5-tetramethyl-1-pyrrolidinyloxy (3AP) spintrap (final concentration = 500  $\mu\text{mol/L}$ ) was also included. A Bruker Elexsys E500 spectrometer equipped with an X-band microwave bridge was used to perform EPR spectroscopy. The concentration of 3AP, as well as EPR instrument parameters, was optimized to obtain the appropriate signal intensity and sensitivity for the TiO<sub>2</sub> NP incubation samples. The following instrument parameters were utilized: microwave power = 2 mW (10 was too high, so it was changed to 2 mW), modulation frequency = 100 kHz, and modulation amplitude = 0.1 mT. The TiO<sub>2</sub> NP samples were incubated in a water bath at 37 °C for at least 1 h before each EPR measurement to mimic the conditions utilized in the DNA damage assays. The incubation/spin trap samples were measured for at least 30 min. Two light conditions were tested: dark exposures with no light added and a laboratory light condition where a special filter was added to the EPR instrument to remove UV light. A 500W xenon arc lamp (Oriel model 66021) equipped with a 90 degree deflecting mirror (Newport model 66246) served as a visible light filter. The arc lamp was positioned 0.6 m from the perforated EPR sample compartment, and the light intensity and distribution that reached the samples was calibrated using the system described in the Protocol for Visible Light Exposure Studies (also see Supporting Information, Figure S1).

**Statistical Analyses.** GraphPad Prism 5.0 software was utilized for statistical analyses. Significant differences were determined by one-way analysis of variance (ANOVA) with posthoc Dunnett's multiple comparison test ( $\alpha = 0.05$ ) between the control samples and the experimental samples in terms of the measured lesion levels. The final data was log-transformed before statistical significance testing because homogeneity of variance (Bartlett's test) was not satisfied in the nontransformed data. The positive control lesion data were included in the ANOVA analyses.

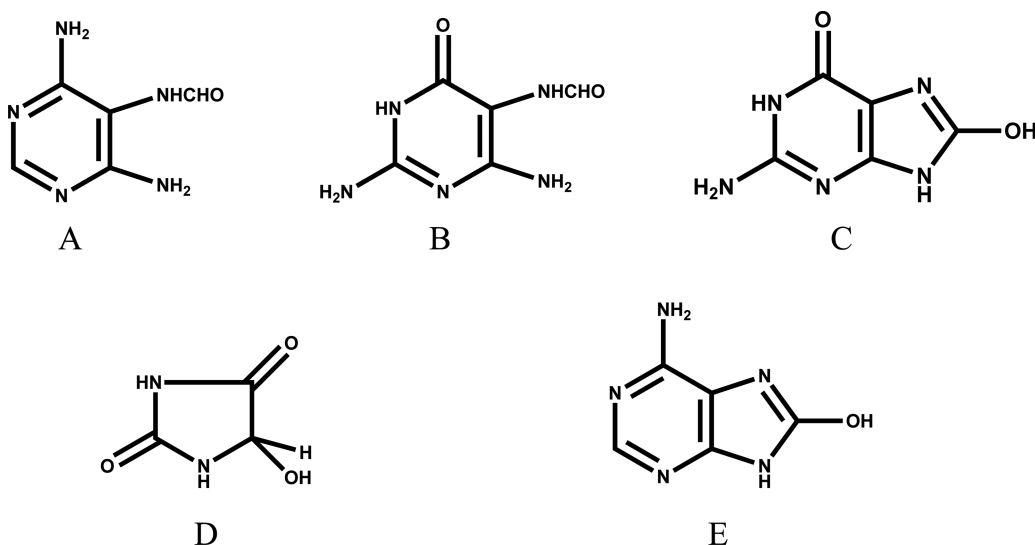


**Figure 2.** Oxidatively modified DNA base lesions investigated in this study: (A) 4,6-diamino-5-formamidopyrimidine (Fapy Adenine), (B) 2,6-diamino-4-hydroxy-5-formamidopyrimidine (Fapy Guanine), (C) 8-hydroxyguanine (8-OH-Guanine), (D) 5-hydroxy-5-methylhydantoin (5-OH-5-MeHyd), and (E) 8-hydroxyadenine (8-OH-Adenine).

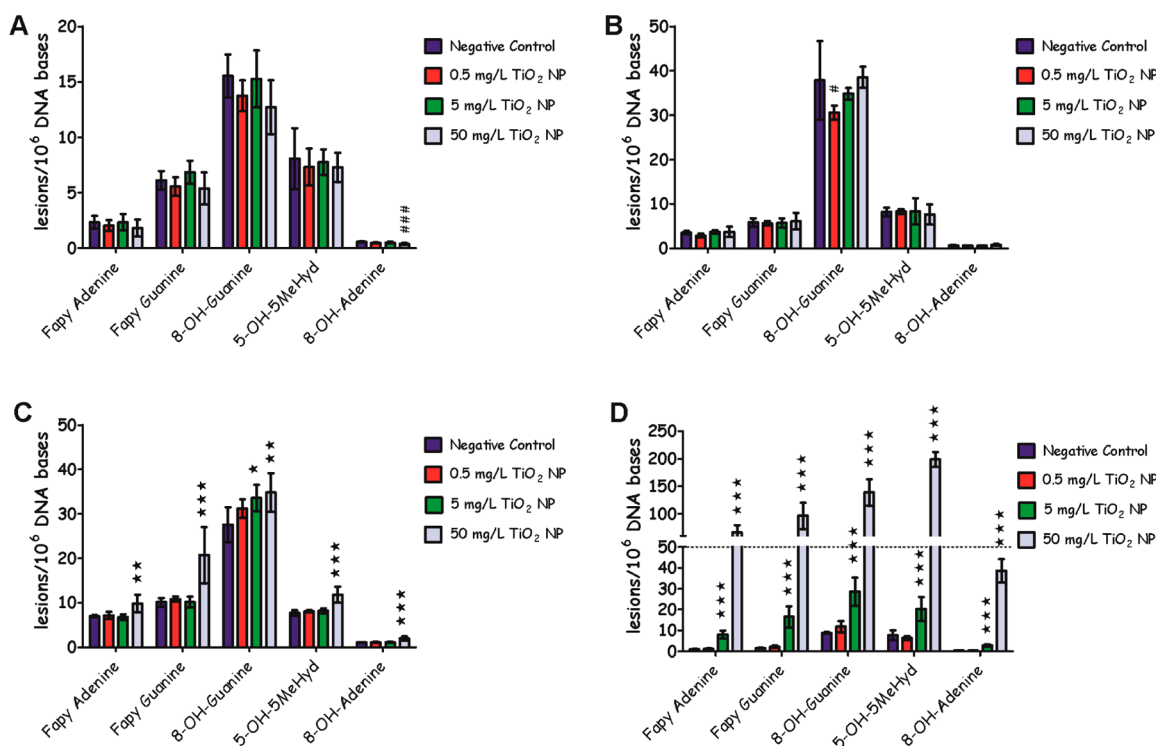


**Figure 3.** DNA base damage profile for ct-DNA exposed to increasing concentrations of P25 TiO<sub>2</sub> NPs (0.5–50 mg/L) after exposure (A) in the dark for 3 h, (B) in the dark for 24 h exposure, (C) using ambient lighting conditions (24 h; 14.5 kJ/m<sup>2</sup>, 400–800 nm), and (D) using UVA irradiation conditions (30 min exposure; 10.0 kJ/m<sup>2</sup>, 370 nm). Number signs (#) indicate statistically significant decreased lesion levels, and asterisks indicate significantly increased lesion level results compared to that of the control samples using one-way analysis of variance (ANOVA) followed by Dunnett's multiple comparison test. One, two, and three asterisks or number signs indicate  $p < 0.05$ , 0.01, and 0.001, respectively. All data points represent the mean of 5 to 6 independent measurements. Uncertainties are standard deviations.

## RESULTS

**Characterization of NP Dispersions.** TiO<sub>2</sub> NP dispersions were tested within a week of every experiment using LDS to ensure that the distribution had not changed. The mean, median, D10, and D90 particle sizes from eight different measurements during the time course of the experiments were  $74.9 \pm 16.0$ ,  $70.8 \pm 2.6$ ,  $59.8 \pm 1.3$ , and  $83.0 \pm 3.9$  nm,,

respectively ( $n = 8$ ; uncertainties represent standard deviations except for the mean in which the error was propagated for the instrument uncertainty and the uncertainty from the replicates). The resulting data indicated that the NP dispersions were stable.

**Dark Exposure Study.** The DNA damage profiles for the 3 and 24 h TiO<sub>2</sub> NP exposures in the dark are shown in Figure 3A,B, respectively; Figure S2A,B includes the data for the 3 and

24 h exposures, respectively, with positive control samples. For both exposure periods, there was no statistically significant formation of oxidatively induced DNA damage in comparison to that of the negative control levels over the tested NP exposure range. LC/MS/MS and GC/MS/MS analyses were also performed on an additional set of samples exposed to TiO<sub>2</sub> NPs for 24 h to confirm the lack of guanine oxidation during the GC/MS/MS analysis procedure. Statistically significant increases in the levels of 8-OH-deoxyguanosine or 8-OH-guanine were not observed after LC/MS/MS or GC/MS/MS analysis (see Figure S3), respectively, and artifactual formation of 8-OH-guanine was not observed.

**Visible Light Exposure Study.** The DNA damage profile for the 24 h TiO<sub>2</sub> NP exposure under ambient light conditions is shown without and with the positive control samples in Figures 3C and S2C, respectively. There was a statistically significant increase in oxidatively induced DNA damage, in comparison to that for the negative control levels, for all five monitored lesions at the highest NP exposure (50 mg/L). For the 8-OH-guanine lesion, there was a distinctive, linear dose–response effect that includes a statistically significant increase in the lesion at the 5 mg/L NP exposure.

**UVA Light Exposure Study.** The DNA damage profile for the 30 min TiO<sub>2</sub> NP exposure under UVA light conditions is shown with and without the positive control samples in 3D and S2D, respectively. There was a dramatic, statistically significant increase in oxidatively induced DNA damage, in comparison to the negative control levels, for all five monitored lesions at both the 5 and 50 mg/L NP exposure levels. Additionally, for all lesions, there was an order of magnitude increase or greater in the absolute number of lesions generated at the 50 mg/L NP exposure level. As observed in the ambient light exposure study, the 8-OH-guanine lesion shows a linearly increasing response in terms of NP dose.

**EPR Spin-Trapping Study.** When TiO<sub>2</sub> NP/ct-DNA samples (50 mg/L TiO<sub>2</sub> NP) were incubated in the dark, there was a slight (~5%) increase, in comparison to  $t = 0$ , in the level of detected free radicals over time (Figure 4). However, when the same samples were incubated under visible light conditions, there was a distinct (~20%) increase, in comparison to  $t = 0$ , in the level of detected free radicals over time (Figure 4). Using linear least-squares regression analysis, the dark and visible light EPR best fit lines (slopes) were significantly differently at the 95% confidence level. This finding indicated

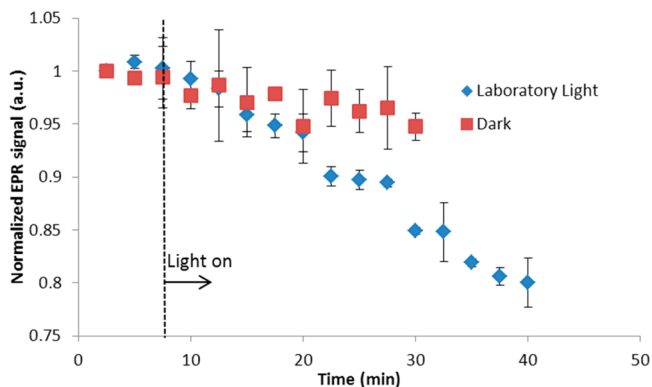


**Figure 4.** EPR spin trapping spectroscopic analysis of 50 mg/L TiO<sub>2</sub> NP/ct-DNA samples under dark and visible light exposure conditions. Data represent means and standard deviations of duplicate measurements.

that the level of free radicals detected under visible light conditions was significantly enhanced in comparison to the level of free radicals detected under the dark conditions in the test samples.

## DISCUSSION

DNA oxidation can result in damage to either the 2'-deoxyribose and/or to the nucleobases in duplex DNA. If the oxidizing species is  $\cdot\text{OH}$ , then both direct SSBs and oxidatively modified DNA bases can be generated. The formation and biological effects of these lesions has been widely investigated.<sup>33</sup> However, not all lesions possess equivalent mutagenic or cytotoxic potential; thus, it is important to identify, quantify, and characterize the likely spectrum of lesions generated under a given exposure scenario. For example, Fapy adenine and Fapy guanine are both purine-derived, imidazole ring-opened compounds that are major promutagenic lesions.<sup>34</sup> Fapy adenine induces A  $\rightarrow$  C transversion mutations and possibly A  $\rightarrow$  T transversion mutations, while Fapy guanine induces G  $\rightarrow$  T transversion mutations. The guanine nucleobase is readily attacked by  $\cdot\text{OH}$  to produce abundant levels of 8-OH-guanine, a lesion that is commonly recognized as both an *in vitro* and *in vivo* biomarker of oxidative stress. 8-OH-guanine is also a mutagenic lesion that induces G  $\rightarrow$  T transversion mutations.<sup>35</sup> The formation and accumulation of 5-OH-5-MeHyd within cells represents a potential lethality; this cytotoxic lesion is a major oxidation decomposition product of thymine and 5-methylcytosine in DNA and acts as a potential block to DNA polymerases.<sup>36,37</sup> Finally, when  $\cdot\text{OH}$  attacks the adenine nucleobase in DNA, the weakly mutagenic 8-OH-adenine lesion forms. Accumulation of 8-OH-adenine induces A  $\rightarrow$  C transversion and A  $\rightarrow$  G transition mutations.<sup>38–40</sup>

In the present study, we have attempted to characterize and understand the lesion generation capacity of commercial P25 TiO<sub>2</sub> NPs under carefully controlled photoactivation conditions. The debate over the type of reactive oxygen species (ROS), if any, generated from both nonphotoactivated and photoactivated TiO<sub>2</sub> NPs in aqueous solution is ongoing. Nevertheless, recent and consistent evidence, based on the use of EPR<sup>2,41</sup> and fluorescence<sup>42</sup> spectroscopy, demonstrate that  $\cdot\text{OH}$  is not produced by TiO<sub>2</sub> NPs at detectable levels when the NPs are incubated in aqueous solutions in the dark. However, when these same aqueous NP solutions are exposed to UVA radiation exceeding the TiO<sub>2</sub> band gap (~400 nm),  $\cdot\text{OH}$  is the only ROS formed at significant levels.<sup>2,41,42</sup> It is known that TiO<sub>2</sub> in dry powder form has a bare surface that can support the catalytic reduction of oxygen to O<sub>2</sub> $\cdot^-$ , as well as other radical reactions, that are independent of dark or UVA exposure.<sup>3,41</sup> The resulting ROS that are formed due to surface catalysis are of such low relative concentration in comparison to those formed from UV irradiation that when the TiO<sub>2</sub> NPs are introduced into an aqueous environment the potential reactivity from these surface ROS becomes negligible. Using acellular, aqueous conditions, we have clearly shown that TiO<sub>2</sub> NPs incubated with DNA in the dark do not lead to statistically significant accumulation (in comparison to that of control samples) of ROS-generated DNA base lesions over a 24 h exposure period (Figures 3A,B and S2A,B). The measured background level of 8-OH-guanine (~35 lesions/10<sup>6</sup> DNA bases) in the control samples for the 24 h incubation study was increased by more than 130% (Figure 3B) in comparison to the

background level of 8-OH-guanine ( $\sim 15$  lesions/ $10^6$  DNA bases) in the 3 h incubation study (Figure 3A). However, this effect was due to a combination of the increased time and oxygen exposure factors during the 24 h incubation period and not due to specific NP interactions with DNA. The guanine base has the lowest reduction potential of the four DNA bases, and guanine is known to readily oxidize to 8-OH-guanine in DNA samples maintained in oxygenated environments.<sup>43</sup>

The majority of the TiO<sub>2</sub> NP/UVA radiation exposure studies reporting DNA damage in the literature utilized radiation doses between 2.5 and  $\geq 275$  kJ/m<sup>2</sup>.<sup>2,7,10,25,27,44</sup> Thus, we chose to investigate the lower portion of the tested dose range ( $\leq 15$  kJ/m<sup>2</sup>) for both the visible and UVA exposure protocols in the present study in order to focus on the potential DNA damage response, if any, resulting from relatively low energy doses. In sharp contrast to the findings for the TiO<sub>2</sub> NP/DNA samples under dark exposure conditions, TiO<sub>2</sub> NP/DNA samples exposed to a low dose (14.5 kJ/m<sup>2</sup>) of visible light radiation generated statistically significant ( $p < 0.01$ ) increases in lesion levels (in comparison to control levels) for all five lesions at the highest (50 mg/L) NP dose (Figure 3C and S2C). In addition, for the 8-OH-guanine lesion, there was a clear dose–response increase in the level of this lesion, which correlated with increasing NP doses. This observation is logical based on the putative visible light photoactivation of TiO<sub>2</sub> NPs<sup>45</sup> to produce  $\bullet$ OH and the subsequent rapid attack and easy oxidation of guanine in DNA by  $\bullet$ OH. However, when comparing the relative DNA lesion increases across all of the detected lesions at the 50 mg/L NP dose, 8-OH-guanine increased the least (26%) and Fapy guanine increased the most (105%), in comparison to control lesion levels. The potential biological relevance of this result (4-fold difference between 8-OH-guanine and Fapy guanine relative accumulation) cannot be understood without evaluating the kinetics of lesion formation under the experimental exposure conditions in an actual cell-based model.

We also determined the spectrum of base lesions resulting from a dose of UVA light (10 kJ/m<sup>2</sup>) using UVA radiation at 370 nm, a wavelength that is less than the band gap excitation wavelength range ( $\lambda = 385$ –410 nm) for P25 TiO<sub>2</sub> NPs.<sup>45</sup> As expected, these conditions resulted in the formation of large, statistically significant ( $p < 0.001$ ) DNA lesion levels in all of the TiO<sub>2</sub> NP/DNA samples at both the 5 and 50 mg/L NP exposure doses (Figures 3D and S2D).

The 3AP spin probe is a nonspecific nitroxide reagent commonly used for trapping free radicals in EPR spectroscopy experiments. The reagent does not inherently possess specificity for oxygen-, carbon-, or nitrogen-centered radical species. Thus, on the basis of the present EPR results (Figure 4), it cannot be definitively concluded that  $\bullet$ OH was the radical species generating the DNA damage profiles shown in Figure 3C,D. However, both the observed pattern and levels of lesions produced during the visible light and UVA exposures are strongly indicative of  $\bullet$ OH attack on DNA.<sup>31</sup> More importantly, even though a low amount of free radical species are found under dark exposure conditions, these radicals do not appear to be capable of promoting oxidatively induced damage to DNA. However, once visible light is introduced into the TiO<sub>2</sub> NP/ct-DNA sample, the level of free radical species generated is high enough that significant oxidatively induced DNA damage is observed.

Our overall results suggest that ordinary room light, i.e., visible light from laboratory fluorescent light bulbs, has the

capacity to photoactivate P25 TiO<sub>2</sub> NPs and induce extensive DNA damage at the molecular level when TiO<sub>2</sub> is present at higher concentrations. Indeed, mixed anatase/rutile crystal phase NPs like P25 have previously been shown to be photoactive in the visible region of the radiation spectrum.<sup>45</sup> Under visible light radiation, the rutile portion of the mixed-crystal P25 lattice (band gap of 3.0 eV and excitation wavelengths that extend into the visible region (410 nm)) acts like an antennae to trap electrons and slow electron–hole recombination. These trapped electrons are then capable of being transferred to the anatase phase, thus maintaining charge separation. In contrast, pure rutile NPs cannot trap electrons and thus are not photoactive in the visible region of the spectrum. Our visible light studies might partly explain some of the controversial comet assay-based *in vitro* results showing the induction and formation of SSBs in cellular samples that were either intentionally kept in the dark or exposed only to ambient (visible) light.<sup>11,13</sup> For example, Gurr et al. utilized the Fpg-modified comet assay to show that BEAS-2B cells exposed to either pure rutile TiO<sub>2</sub> NPs or to a 50:50 (volume fraction) mixture of anatase/rutile TiO<sub>2</sub> NPs (10 mg/L) in the dark could accumulate statistically higher levels of SSBs than that of untreated control cells.<sup>13</sup> The measured Fpg-induced SSBs directly correlate to the presence of oxidatively induced DNA base lesions (8-OH-guanine, Fapy adenine, etc.) in the cells. Our GC/MS/MS and EPR data suggest that these lesions are not formed to any significant extent in the dark. Thus, it is feasible that the cells in the Gurr study were either exposed to visible light and/or that a NP-induced inflammatory response and increase in ROS level was responsible for the reported DNA damage. Recently, Gerloff et al. showed Fpg-modified comet assay results for Caco-2 cells exposed to P25 TiO<sub>2</sub> NPs (20  $\mu$ g/cm<sup>2</sup>) under dark conditions.<sup>11</sup> The authors found that there was a slight (nonsignificant) increase in the level of detected SSBs for TiO<sub>2</sub> NP exposed cells when the comet assay samples were processed in the dark. However, the increased level of SSBs for cells exposed to TiO<sub>2</sub> NPs under identical culture conditions became statistically significant when the comet assay was conducted under normal laboratory lighting conditions. These results directly support our DNA base lesion results for both the dark and visible light exposure conditions. In our dark exposure studies (Figure 3A,B), we observed an increase in the background levels for 8-OH-guanine, depending on the length of the sample incubation period (3 or 24 h), but there was not a significant difference in the lesion levels for samples incubated with or without TiO<sub>2</sub>. In contrast, the measured 8-OH-guanine level became statistically significantly increased for samples with TiO<sub>2</sub> after visible light radiation (Figure 3C).

Furthermore, our data clearly shows that 8-OH-guanine is not the only biologically relevant lesion formed due to visible or UVA light induced TiO<sub>2</sub> NP photoactivation. Previous *in vivo* and *in vitro* TiO<sub>2</sub> NP exposure studies<sup>27,46,47</sup> have measured only 8-OH-guanine or 8-OH-deoxyguanine to the potential exclusion of other lesions that could evince equal or greater mutagenicity or cytotoxicity depending on exposure conditions. In our exposure models, the relative formation and accumulation of 8-OH-guanine in the NP samples was lower than the formation and accumulation of the other four lesions. The accumulation of any of the measured lesions in cells can result in SSBs in the DNA molecule based solely on base excision repair processes; thus, it is important to identify and quantitatively measure more than 8-OH-guanine alone.

Previously, it was reported that photoirradiated TiO<sub>2</sub> NPs could lead to site-specific guanine and thymine cleavages in ct-DNA due to the generation and accumulation of oxidatively modified guanine and thymine bases.<sup>25</sup> The authors hypothesized that guanine and thymine lesions could be formed in ct-DNA at significant levels. We have now demonstrated, at the molecular level, that photoactivated P25 TiO<sub>2</sub> NPs can induce a wide spectrum of measurable and discrete thymine, guanine, and adenine base lesions.

In closing, our experiments demonstrate that P25 TiO<sub>2</sub> NPs incubated with duplex DNA in the dark do not lead to the formation of DNA base lesions. However, when the same samples are exposed to either visible light from 400 to 800 nm (energy dose = 14.5 kJ/m<sup>2</sup>) or UVA light at 370 nm (energy dose = 10 kJ/m<sup>2</sup>), a wide spectrum of potentially cytotoxic and/or mutagenic DNA base lesions are generated at statistically significant levels, dependent on the NP concentration in solution. The presented data suggests that commercial P25 TiO<sub>2</sub> NPs do not have an inherent capacity to oxidatively damage DNA bases in the absence of sufficient photoactivation. However, radiation within the visible portion of the electromagnetic radiation spectrum has the potential to induce the formation of DNA base lesions and thus DNA SSBs. The observed DNA damage appears to be mediated and promoted by TiO<sub>2</sub> NP induced •OH formation. Future studies using the comet assay to assess SSBs after exposing cells to TiO<sub>2</sub> NPs should conduct the processing steps in the dark to minimize potential artifacts from laboratory light and should report the conditions used during the processing steps. Understanding potential artifacts in nanotoxicology experiments is critical for providing reliable data and accurate risk assessment.<sup>48</sup>

## ■ ASSOCIATED CONTENT

### ■ Supporting Information

Spectral profile of the NIST calibrated halogen lamp, a DNA base damage profiles with positive control samples included for the TiO<sub>2</sub> NP exposure samples, profile of DNA nucleoside damage (8-OH-deoxyguanosine) and DNA base damage (8-OH-guanine) after 24 h dark exposure using LC/MS/MS and GC/MS/MS, respectively, methods for verification of removal of TiO<sub>2</sub> NPs by centrifugation, detailed description of the DNA enzymatic digestion procedure and GC/MS/MS methodology utilized in the present study, and detailed description of the isotope-dilution LC/MS/MS methodology utilized for the determination of 8-OH-deoxyguanosine levels. This material is available free of charge via the Internet at <http://pubs.acs.org>.

## ■ AUTHOR INFORMATION

### Corresponding Author

\*E-mail: [bryant.nelson@nist.gov](mailto:bryant.nelson@nist.gov). Phone: 301-975-2517. Fax: 301-975-8246.

### Funding

The authors declare no outside funding sources.

### Notes

Certain commercial equipment, instruments, and materials are identified in this article to specify an experimental procedure as completely as possible. In no case does the identification of particular equipment or materials imply a recommendation or endorsement by the National Institute of Standards and Technology nor does it imply that the materials, instruments, or equipment are necessarily the best available for the purpose.

The authors declare no competing financial interest.

## ■ ACKNOWLEDGMENTS

We thank Julian Taurozzi and Vince Hackley of NIST for their helpful advice and discussions regarding the dispersion and characterization of the P25 TiO<sub>2</sub> NPs (NIST SRM 1898) utilized in this study and for use of their LDS. We also thank Pawel Jaruga of NIST for his continuous technical help and assistance with the mass spectrometry instrumentation.

## ■ REFERENCES

- (1) Weir, A., Westerhoff, P., Fabricius, L., Hrisotovski, K., and Von Goetz, N. (2012) Titanium dioxide nanoparticles in food and personal care products. *Environ. Sci. Technol.* 46, 2242–2250.
- (2) Dodd, N. J. F., and Jha, A. N. (2011) Photoexcitation of aqueous suspensions of titanium dioxide nanoparticles: an electron spin resonance spin trapping study of potentially oxidative reactions. *Photochem. Photobiol.* 87, 632–640.
- (3) Fujishima, A., Rao, T. N., and Tryk, D. A. (2000) Titanium dioxide photocatalysis. *J. Photochem. Photobiol., C* 1, 1–21.
- (4) Petersen, E. J., and Nelson, B. C. (2010) Mechanisms and measurements of nanomaterial-induced oxidative damage to DNA. *Anal. Bioanal. Chem.* 398, 613–650.
- (5) Tran, D. T., and Salmon, R. (2011) Potential photocarcinogenic effects of nanoparticle sunscreens. *Australas. J. Dermatol.* 52, 1–6.
- (6) Dizdaroglu, M., Jaruga, P., Birincioglu, M., and Rodriguez, H. (2002) Free radical-induced damage to DNA: mechanisms and measurement. *Free Radical Biol. Med.* 32, 1102–1115.
- (7) Nakagawa, Y., Wakuri, S., Sakamoto, K., and Tanaka, K. (1997) The photogenotoxicity of titanium dioxide particles. *Mutat. Res.* 394, 125–132.
- (8) Dunford, R., Salinaro, A., Cai, L., Serpone, N., Horikoshi, S., Hidaka, H., and Knowland, J. (1997) Chemical oxidation and DNA damage catalyzed by inorganic sunscreen ingredients. *FEBS Lett.* 418, 87–90.
- (9) Serpone, N., Salinaro, A. E., Horikoshi, S., and Hidaka, H. (2006) Beneficial effects of photo-inactive titanium dioxide specimens on plasmid DNA, human cells and yeast cells exposed to UVA/UVB simulated sunlight. *J. Photochem. Photobiol., A* 179, 200–212.
- (10) Reeves, J. F., Davies, S. J., Dodd, N. J. F., and Jha, A. N. (2008) Hydroxyl radicals are associated with titanium dioxide (TiO<sub>2</sub>) nanoparticle-induced cytotoxicity and oxidative DNA damage in fish cells. *Mutat. Res.* 640, 113–122.
- (11) Gerloff, K., Albrecht, C., Boots, A. W., Forster, I., and Schins, R. P. F. (2009) Cytotoxicity and oxidative DNA damage by nanoparticles in human intestinal Caco-2 cells. *Nanotoxicology* 3, 355–364.
- (12) Guichard, Y., Schmit, J., Darne, C., Gate, L., Goutet, M., Rousset, D., Rastoix, O., Wrobel, R., Witschger, O., Martin, A., Fierro, V., and Binet, S. (2012) Cytotoxicity and genotoxicity of nanosized and micro-sized titanium dioxide and iron oxide particles in syrian hamster embryo cells. *Ann. Occup. Hyg.* 56, 631–644.
- (13) Gurr, J. R., Wang, A. S. S., Chen, C. H., and Jan, K. Y. (2005) Ultrafine titanium dioxide particles in the absence of photoactivation can induce oxidative damage to human bronchial epithelial cells. *Toxicology* 213, 66–73.
- (14) Kang, S. J., Kim, B. M., Lee, Y. J., and Chung, H. W. (2008) Titanium dioxide nanoparticles trigger p53-mediated damage response in peripheral blood lymphocytes. *Environ. Mol. Mutagen.* 49, 399–405.
- (15) Shukla, R. K., Kumar, A., Gurbani, D., Pandey, A. K., Singh, S., and Dhawan, A. (2013) TiO<sub>2</sub> nanoparticles induce oxidative DNA damage and apoptosis in human liver cells. *Nanotoxicology* 7, 48–60.
- (16) Hackenberg, S., Friehs, G., Kessler, M., Froelich, K., Ginzkey, C., Koehler, C., Scherzed, A., Burghartz, M., and Kleinsasser, N. (2011) Nanosized titanium dioxide particles do not induce DNA damage in human peripheral blood lymphocytes. *Environ. Mol. Mutagen.* 52, 264–268.
- (17) Woodruff, R. S., Li, Y., Yan, J., Bishop, M., Jones, M. Y., Watanabe, F., Biris, A. S., Rice, P., Zhou, T., and Chen, T. (2012)

Genotoxicity evaluation of titanium dioxide nanoparticles using the Ames test and Comet assay. *J. Appl. Toxicol.* 32, 934–943.

(18) Rajapakse, K., Drobne, D., Kastelec, D., and Marinsek-Logar, R. (2013) Experimental evidence of false-positive Comet test results due to TiO<sub>2</sub> particle-assay interactions. *Nanotoxicology* 7, 1043–1051.

(19) Lin, M. H., Hsu, T. S., Yang, P. M., Tsai, M. Y., Perng, T. P., and Lin, L. Y. (2009) Comparison of organic and inorganic germanium compounds in cellular radiosensitivity and preparation of germanium nanoparticles as a radiosensitizer. *Int. J. Radiat. Biol.* 85, 214–226.

(20) Atha, D. H., Wang, H., Petersen, E. J., Cleveland, D., Holbrook, R. D., Jaruga, P., Dizdaroglu, M. M., Xing, B., and Nelson, B. C. (2012) Copper oxide nanoparticle mediated DNA damage in terrestrial plant models. *Environ. Sci. Technol.* 46, 1819–1827.

(21) Hunt, P. R., Marquis, B. J., Tyner, K. M., Conklin, S., Olejnik, N., Nelson, B. C., and Sprando, R. L. (2013) Nanosilver suppresses growth and induces oxidative damage to DNA in *Caenorhabditis elegans*. *J. Appl. Toxicol.* 33, 1131–1142.

(22) Nelson, B. C., Petersen, E. J., Marquis, B. J., Atha, D. H., Elliott, J. T., Cleveland, D., Watson, S. S., Tseng, I. H., Dillon, A., Theodore, M., and Jackman, J. (2013) NIST gold nanoparticle reference materials do not induce oxidative DNA damage. *Nanotoxicology* 7, 21–29.

(23) Petersen, E. J., Tu, X., Dizdaroglu, M., Zheng, M., and Nelson, B. C. (2013) Protective roles of single wall carbon nanotubes in ultrasonication-induced DNA damage. *Small* 9, 205–208.

(24) Singh, N., Jenkins, G. J., Nelson, B. C., Marquis, B. J., Maffei, T. G., Brown, A. P., Williams, P. M., Wright, C. J., and Doak, S. H. (2012) The role of iron redox state in the genotoxicity of ultrafine superparamagnetic iron oxide nanoparticles. *Biomaterials* 33, 163–170.

(25) Hirakawa, K., Mori, M., Yoshida, M., Oikawa, S., and Kawanishi, S. (2004) Photo-irradiated titanium dioxide catalyzes site specific DNA damage via generation of hydrogen peroxide. *Free Radical Res.* 38, 439–447.

(26) Kemp, T. J., and McIntyre, R. A. (2007) Photodegradation of DNA induced by modified forms of titanium dioxide. *Prog. React. Kinet. Mech.* 32, 219–229.

(27) Wamer, W. G., Yin, J. J., and Wei, R. R. (1997) Oxidative damage to nucleic acids photosensitized by titanium dioxide. *Free Radical Biol. Med.* 23, 851–858.

(28) Hidaka, H., Horikoshi, S., Serpone, N., and Knowland, J. (1997) In vitro photochemical damage to DNA, RNA and their bases by an inorganic sunscreen agent on exposure to UVA and UVB radiation. *J. Photochem. Photobiol., A* 111, 205–213.

(29) NIST Standard Reference Material 1898, Titanium Dioxide Nanomaterial, Certificate of Analysis. [https://www-s.nist.gov/srmors/view\\_cert.cfm?srm=1898](https://www-s.nist.gov/srmors/view_cert.cfm?srm=1898) (accessed February 2013).

(30) Taurozzi, J. S., Hackley, V. A., and Wiesner, M. R. (2013) A standardised approach for the dispersion of titanium dioxide nanoparticles in biological media. *Nanotoxicology* 7, 389–401.

(31) Aruoma, O. I., Halliwell, B., Gajewski, E., and Dizdaroglu, M. (1991) Copper-ion-dependent damage to the bases in DNA in the presence of hydrogen-peroxide. *Biochem. J.* 273, 601–604.

(32) Rodriguez, H., Jurado, J., Laval, J., and Dizdaroglu, M. (2000) Comparison of the levels of 8-hydroxyguanine in DNA as measured by gas chromatography mass spectrometry following hydrolysis of DNA by *Escherichia coli* Fpg protein or formic acid. *Nucleic Acids Res.* 28, 1–8.

(33) Evans, M. D., Dizdaroglu, M., and Cooke, M. S. (2004) Oxidative DNA damage and disease: induction, repair and significance. *Mut. Res.* 567, 1–61.

(34) Dizdaroglu, M., Kirkali, G., and Jaruga, P. (2008) Formamidopyrimidines in DNA: mechanisms of formation, measurement, repair and biological effects. *Free Radical Biol. Med.* 45, 1610–1621.

(35) Demple, B., and Harrison, L. (1994) Repair of oxidative damage to DNA: enzymology and biology. *Annu. Rev. Biochem.* 63, 915–948.

(36) Gasparutto, D., Ait-Abbas, M., Jaquinod, M., Boiteux, S., and Cadet, J. (2000) Repair and coding properties of 5-hydroxy-5-methylhydantoin nucleosides inserted into DNA oligomers. *Chem. Res. Toxicol.* 13, 575–584.

(37) Redrejo-Rodriguez, M., Saint-Pierre, C., Couve, S., Mazouzi, A., Ishchenko, A. A., Gasparutto, D., and Saparbaev, M. (2011) New insights in the removal of the hydantoins, oxidation product of pyrimidines, via the base excision and nucleotide incision repair pathways. *PLoS One* 6, e21039.

(38) Grin, I. R., Dianov, G. L., and Zharkov, D. O. (2010) The role of mammalian NEIL1 protein in the repair of 8-oxo-7,8-dihydroadenine in DNA. *FEBS Lett.* 584, 1553–1557.

(39) Kalam, M. A., Haraguchi, K., Chandani, S., Loechler, E. L., Moriya, M., Greenberg, M. M., and Basu, A. K. (2006) Genetic effects of oxidative DNA damages: comparative mutagenesis of the imidazole ring-opened formamidopyrimidines (Fapy lesions) and 8-oxo-purines in simian kidney cells. *Nucleic Acids Res.* 34, 2305–2315.

(40) Kamiya, H., Miura, H., Murata-Kamiya, N., Ishikawa, H., Sakaguchi, T., Inoue, H., Sasaki, T., Masutani, C., Hanaoka, F., Nishimura, S., et al. (1995) 8-Hydroxyadenine (7,8-dihydro-8-oxoadenine) induces misincorporation in *in vitro* DNA synthesis and mutations in NIH 3T3 cells. *Nucleic Acids Res.* 23, 2893–2899.

(41) Fenoglio, I., Greco, G., Livraghi, S., and Fubini, B. (2009) Non-UV-induced radical reactions at the surface of TiO<sub>2</sub> nanoparticles that may trigger toxic responses. *Chemistry* 15, 4614–4621.

(42) Ma, H., Brennan, A., and Diamond, S. A. (2012) Photocatalytic reactive oxygen species production and phototoxicity of titanium dioxide nanoparticles are dependent on the solar ultraviolet radiation spectrum. *Environ. Toxicol. Chem.* 31, 2099–2107.

(43) Steenken, S. (1989) Purine bases, nucleosides and nucleotides: aqueous solution redox chemistry and transformation reactions of their radical cations and electron and hydroxyl radical adducts. *Chem. Rev.* 89, 503–520.

(44) Tiano, L., Armeni, T., Venditti, E., Barucca, G., Mincarelli, L., and Damiani, E. (2010) Modified TiO<sub>2</sub> particles differentially affect human skin fibroblasts exposed to UVA light. *Free Radical Biol. Med.* 49, 408–415.

(45) Hurum, D. C., Agrios, A. G., Gray, K. A., Rajh, T., and Thurnauer, M. C. (2003) Explaining the enhanced photocatalytic activity of Degussa P25 mixed-phase TiO<sub>2</sub> using EPR. *J. Phys. Chem. B* 107, 4545–4549.

(46) Bhattacharya, K., Davoren, M., Boertz, J., Schins, R. P. F., Hoffmann, E., and Dopp, E. (2009) Titanium dioxide nanoparticles induce oxidative stress and DNA-adduct formation but not DNA-breakage in human lung cells. *Part. Fibre Toxicol.* 6, 17.

(47) Trouiller, B., Reliene, R., Westbrook, A., Solaimani, P., and Schiestl, R. H. (2009) Titanium dioxide nanoparticles induce DNA damage and genetic instability *in vivo* in mice. *Cancer Res.* 69, 8784–8789.

(48) Petersen, E. J., Henry, T. B., Zhao, J., MacCuspie, R. I., Kirschling, T. L., Dobrovolskaia, M. A., Hackley, V., Xing, B., and White, J. C. (2014) Identification and avoidance of potential artifacts and misinterpretations in nanomaterial ecotoxicity measurements. *Environ. Sci. Technol.* 48, 4226–4246.